Proc. Natl. Acad. Sci. USA
Vol. 93, pp. 1270–1275, February 1996
Neurobiology

Neuronal abnormalities in microtubule-associated protein 1B mutant mice

(gene targeting/ataxia/Purkinje cells/ocular abnormalities)

WINFRIED EDELMANN*, MARK ZERVAS†, PAMELA COSTELLO‡, LINDA ROBACK†, ITZHAK FISCHER§, JAMES A. HAMMARBACK¶, NICHOLAS COWAN‖, PETER DAVIES**, BRUCE WAINER†, AND RAJU KUCHERLAPATI*

Departments of *Molecular Genetics, †Pathology, ‡Neurosurgery, and **Pathology and Neuroscience, Albert Einstein College of Medicine, 1300 Morris Park Avenue, Bronx, NY 10461; §Department of Anatomy and Neurobiology, Medical College of Pennsylvania and Hahneman University, 3200 Henry Avenue, Philadelphia, PA 19129; ¶Department of Neurobiology and Anatomy, Bowman Gray School of Medicine, Wake Forest University, Winston-Salem, NC 27157; and ‖Department of Biochemistry, New York University, 550 First Avenue, New York, NY 10016

Communicated by Dominick P. Purpura, Albert Einstein College of Medicine, Bronx, NY, October 3, 1995 (received for review May 12, 1995)

ABSTRACT **Microtubules play an important role in establishing cellular architecture. Neuronal microtubules are considered to have a role in dendrite and axon formation. Different portions of the developing and adult brain microtubules are associated with different microtubule-associated proteins (MAPs). The roles of each of the different MAPs are not well understood. One of these proteins, MAP1B, is expressed in different portions of the brain and has been postulated to have a role in neuronal plasticity and brain development. To ascertain the role of MAP1B, we generated mice which carry an insertion in the gene by gene-targeting methods. Mice which are homozygous for the modification die during embryogenesis. The heterozygotes exhibit a spectrum of phenotypes including slower growth rates, lack of visual acuity in one or both eyes, and motor system abnormalities. Histochemical analysis of the severely affected mice revealed that their Purkinje cell dendritic processes are abnormal, do not react with MAP1B antibodies, and show reduced staining with MAP1A antibodies. Similar histological and immunochemical changes were observed in the olfactory bulb, hippocampus, and retina, providing a basis for the observed phenotypes.**

The 255-kDa microtubule-associated protein (MAP) 1B (MAP1B) is a member of a group of proteins that are predominantly associated with microtubules in neurons and glia (1, 2). MAP1B is a complex of three proteins of which two, the heavy chain and a light chain (LC1), are derived respectively from the N terminus (amino acids 2201–2216) and the C terminus (amino acids 247–262) of a polyprotein precursor (3–5). The heavy chain contains an N-terminal LC1-binding domain, a microtubule-binding domain (amino acids 589–787), and a relatively large negatively charged C-terminal region which forms filamentous bridges between adjacent microtubules (1–6). MAP1B is expressed at high levels during embryogenesis and peaks at 2–3 days after birth. Two to three weeks after birth, the expression of MAP1B decreases and expression of other MAPs such as MAP1A increases (7–9). During development this protein is found in areas which show extensive axonal growth, including motor neurons, retinal ganglion cells, olfactory epithelium, the nerve layer of the olfactory bulb, and the mossy fibers of the hippocampus (10–13). In adult brain, MAP1B is found in selected areas where there is active neuronal outgrowth, including the olfactory bulb and regions of the brain where neuronal plasticity may have a role such as the hippocampus as well as in the dendrites of Purkinje cells in the cerebellum (6, 9). Although the patterns of expression of MAP1B *in vivo* and experiments with cultured pheochromocytoma (PC12) cells suggest an important role for this protein in axonal and neurite outgrowth (14–16), there is no definitive information concerning its function in normal growth and development. To examine the role of MAP1B we introduced a targeted mutation in the *Map1b* gene of the mouse. We show that this mutation in the homozygous state results in embryonic lethality, and a subset of the heterozygous animals exhibit a spectrum of neurological phenotypic abnormalities including loss of visual acuity, ataxic gait, spastic tremor of the hindlimbs, and an overall reduction in body weight of up to 50%. Immunohistochemical analysis of the affected animals revealed significant changes in MAP1B protein expression in several parts of the brain.

MATERIALS AND METHODS

Gene Targeting. For the construction of the *Map1b* targeting vector, an 8-kb *Dra* I fragment containing the *Map1b* gene subcloned in the *Sma* I site of pUC8 was used. The resulting targeting vector contained a 1.7-kb PGK Neo cassette in reverse transcriptional orientation, blunt-end inserted into the *Spe* I site 5′ to the region corresponding to the microtubule-binding motif with an 876-bp *Xmn* I–*Spe* I fragment as the 5′ arm and a 6.5-kb *Spe* I–*Dra* I fragment as the 3′ arm. A 1.1-kb *Sal* I–*Xho* I MC1TK cassette (17) was inserted into the unique *Sal* I site at the 5′ end of this clone. The targeting vector was linearized at the unique *Sal* I site and electroporated into E14-1 mouse embryonic stem cells. The cells were selected with G418 and ganciclovir (200 μg/ml and 2 μM, respectively) for 10–14 days. Doubly resistant colonies were isolated and analyzed for homologous recombination events by PCR. The sequences of the primers used for PCR are as follows: 5′ primer, 5′-TCTCCAAGCCTTGCTGTTAC-3′ and the 3′ primer, 5′-CTGCTCTTTACTGAAGGCTC-3′. Conditions for the PCR were 1 cycle at 94°C for 5 min; 60 cycles with 1 min at 94°C, 1 min at 58°C, and 1.5 min at 72°C; and 1 cycle at 72°C for 10 min in 1× *Taq* polymerase buffer (Boehringer Mannheim) with 1.5 mM $MgCl_2$ each of the four dNTPs at 200 μM, each primer at 5 ng/μl, and 2.5 units of *Taq* DNA polymerase (Boehringer Mannheim) in a final volume of 50 μl. After 30 cycles another 2.5 units of *Taq* polymerase was added. Cells from two mouse cell lines (M3407 and M5309) were injected into C57BL/6J mouse blastocysts to generate chimeric animals. Chimeric males were mated with C57BL/6J females to assess germ-line transmission of the embryonic stem cell genome.

Histology. Brains from 5-month-old animals were fixed in 4% paraformaldehyde/0.1% glutaraldehyde solution in 0.1 M

The publication costs of this article were defrayed in part by page charge payment. This article must therefore be hereby marked "*advertisement*" in accordance with 18 U.S.C. §1734 solely to indicate this fact.

Abbreviations: MAP, microtubule-associated protein; MAP1A, MAP1B, and MAP2, MAPs 1A, 1B, and 2; LC1, LC2, etc., light chain 1, light chain 2, etc.

sodium phosphate buffer, pH 7.4. This material was embedded in paraffin, and 10-μm sections were prepared and stained with cresyl violet.

Immunohistochemistry. For immunohistochemistry, adult animals were anesthetized and perfused intracardially with Tyrode's solution, then 4% paraformaldehyde/0.1% glutaraldehyde solution in pH 7.4 phosphate buffer, followed by brief perfusions with 10% and 30% sucrose solutions. The brains were immersed overnight in 30% sucrose. Sections 50 μm thick were cut sagitally through the cerebellum on a freezing microtome. Similar-thickness coronal sections were obtained for the other parts of the brain. The sections were rinsed in 0.01 M phosphate-buffered saline (PBS), pH 7.4, treated with 0.3% H_2O_2 in PBS, then incubated for 1 hr in 5% milk solids/0.1% Triton X-100 in PBS. The sections were incubated with primary antibody in 5% milk solids/PBS overnight at 4°C. The MAP1B antibodies, 3G5 and 6D4, were provided by Lester Binder (University of Alabama). 3G5 is directed against a nonphosphorylated epitope and 6D4 detects a phosphorylated epitope. The MAP1A antibody is a mouse monoclonal purchased from Sigma. On the following day, the sections were processed with a mouse IgG Vectastain Elite kit (Vector Laboratories) and visualized with diaminobenzidine.

Antibodies. Monoclonal antibodies 3G5 (MAP1B), AP14 (MAP2) and Alz50 were used to visualize cytoskeletal proteins after transfer to nitrocellulose. Alz50 reacts with all forms of tau and has some cross-reactivity with MAP2 (18), as well as with a 120-kDa protein we have termed FAC. LC1 and LC2 antigens were purified from taxol-assembled rat brain microtubules by SDS/PAGE. Production of rabbit antiserum to LC3 expressed in *Escherichia coli* was previously described (19). Polypeptide composed of the first 150 amino acids of mouse MAP1B fused to glutathione *S*-transferase was expressed in bacteria and affinity purified on a glutathione column. The affinity-purified fusion protein was used to prepare rabbit antiserum (MAP1B489-3) recognizing the N-terminal region of mouse MAP1B. To obtain antibodies to LC proteins, New Zealand White rabbits were immunized and bled by standard techniques. Tubulin was detected with a commercially available mouse monoclonal antibody to α-tubulin (clone DM1A, Sigma).

Detection of Proteins. For results shown in Fig. 5*a*, dissected cerebella were homogenized in 25 mM Tris·HCl, pH 7.4, containing 25 μM leupeptin, 1 mM EGTA, 1 mM phenylmethanesulfonyl fluoride, and 2% (vol/vol) 2-mercaptoethanol prior to heating at 98°C for 10 min. After removal of precipitated proteins by centrifugation, heat-stable proteins were analyzed on 10% polyacrylamide gels in the presence of SDS. For results shown in Fig. 5*b*, whole brain extracts were dissolved in SDS-containing buffer and electrophoresed on SDS/5–16% polyacrylamide gels and blotted onto nitrocellulose filters. Immunoblotting was performed by conventional methods.

RESULTS

Generation of Mice Carrying a Mutation in the *Map1b* Locus. To generate mice carrying a mutation in the *Map1b* gene we constructed a gene-targeting vector by introducing a neomycin phosphotransferase (neo) expression cassette into a fragment of the cloned genomic locus of mouse *Map1b* (ref. 17; Fig. 1*a*). If the neo cassette-containing sequence integrated into the genomic locus, it would create a premature termination codon corresponding to codon 571 of the *Map1b* coding region. The gene targeting vector was introduced into mouse embryonic stem cell line E14-1 by electroporation. Colonies which grew in the presence of G418 and gancyclovir were isolated, grown, and examined for the desired gene modification initially by a PCR-based method using a primer located in the neo cassette and then by a second primer in genomic DNA outside the region of homology between the target and input DNA (Fig. 1*a*). On the basis of this analysis we obtained three targeted cell lines from the analysis of 744 doubly selected clones, yielding an overall targeting efficiency of 1/670. These

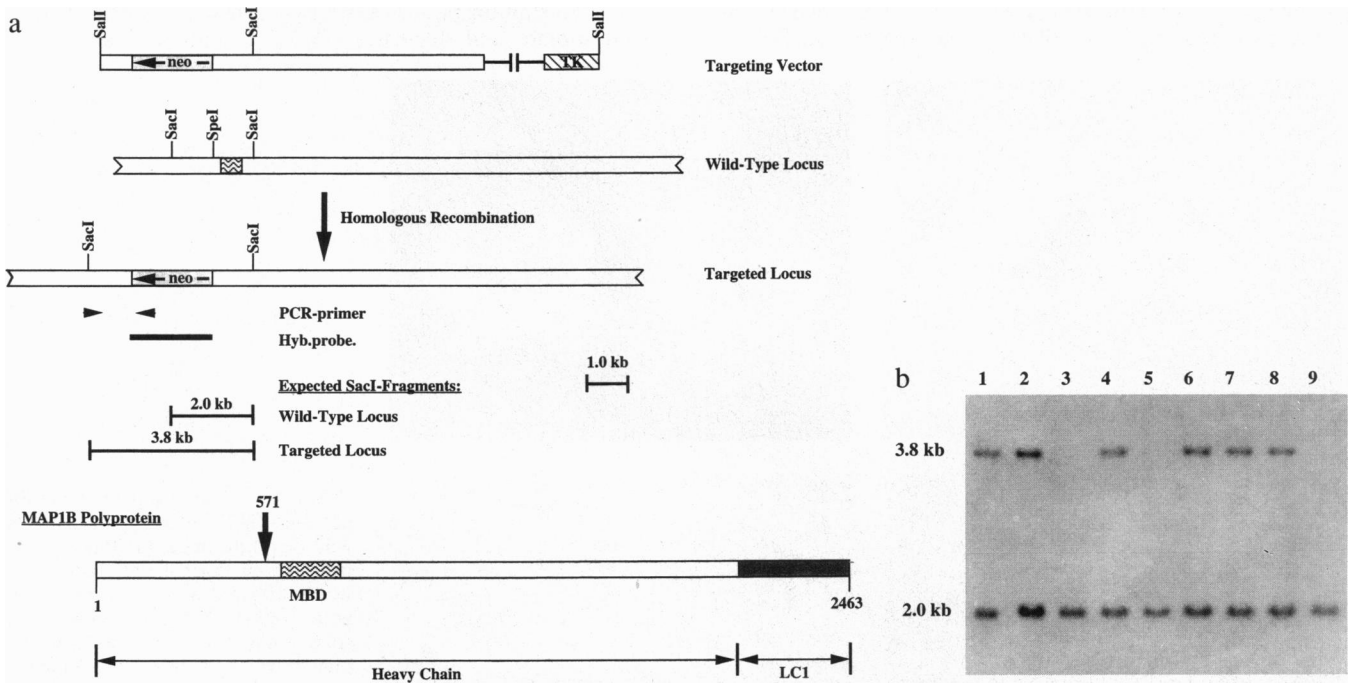

FIG. 1. Generation of mice carrying a mutation at the *Map1b* locus. (*a*) Scheme for generating a gene-targeted disruption of the *Map1b* gene. The structure of the protein product, targeting vector, wild-type *Map1b* locus, and the predicted product of gene targeting are shown. The probes used for detection and the sizes of products detected by the different probes are also shown. TK, thymidine kinase expression cassette; neo, neomycin phosphotransferase expression cassette; MBD, microtubule-binding domain. (*b*) Southern-blot hybridization of DNA from tails of F_1 animals, using the probe shown in *a*. *Sac* I-digested DNA from members of one litter. The 3.8-kb band corresponds to the modified *Map1b* allele and the 2.0-kb band corresponds to the wild-type allele.

cell lines were grown and their DNA was used for Southern-blot hybridization. These results (not shown) confirmed that all of them had undergone a gene-targeting event. Two separate cell lines (M3407 and M5309), derived from independent gene-targeting events, were used to generate chimeric mice by injection into embryos derived from C57BL/6J (B6) animals. Chimeric males were, in turn, mated with B6 females, and germ-line transmission of the embryonic stem cell genome was assessed by coat color of the resulting offspring. Fourteen of the 16 chimeric males transmitted the embryonic stem cell genome through their germ line. DNA from these F_1 animals was examined to determine if any of them contained the modified *Map1b* allele. Results from one such experiment are shown in Fig. 1*b*. All of the animals contained a 2.0-kb band corresponding to the normal locus. Several of the animals (lanes 1, 2, 4, 6, 7, and 8) also contained a second band at 3.8 kb corresponding to the modified allele. These mice are heterozygous for the *Map1b* modification designated *Map1b571*. The heterozygous mice were interbred and the heterozygous F_2 offspring were used for the analyses described below.

Phenotypes of *Map1b571* Heterozygotes. To understand the phenotypic effects of the mutated *Map1b* allele, we followed the heterozygous animals and their wild-type littermates for more than a year. It should be noted that all of these animals had variable genetic contributions from the 129/J and C57BL/6J strains of mice. We observed that the heterozygous animals of both sexes, of various ages, as a group were inhibited in their growth as determined by the fact that they weighed 10–50% less than their age- and sex-matched wild-type littermates (Fig. 2*a*). Twenty-eight of the 140 heterozygous animals (20%) had gross deformities of the ocular orbs. In some animals only one orb was affected, while in others both orbs were affected. Those mice which exhibited disorders of both orbs failed to respond to visual threats, suggesting that they have lost their visual acuity. This subset of heterozygous animals also exhibited a number of other distinctive phenotypic characteristics and were lethargic in their movement, exhibited an ataxic gait, and had a mild to severe spastic tremor of the hind limbs suggestive of cerebellar dysfunction. Some of these animals, later in their life, became paralyzed in their hind limbs, leading to starvation and/or dehydration and death. Among the affected animals the degree of severity of these phenotypes was variable. None of the wild-type littermates had any of these phenotypes. These results suggest that the *Map1b* mutation we introduced is capable of acting in a dominant fashion with variable expressivity.

To ascertain the anatomical basis for the phenotypes observed, we dissected the whole brains of several heterozygous animals and examined them for possible gross morphological abnormalities. The phenotypically abnormal animals had abnormalities in the shape and size of the cerebellum; notably, an attenuated, flattened cerebellar hemisphere and vermis in comparison with wild-type littermates (Fig. 2*b*). An enlargement of the olfactory bulb was observed in a few cases. The hippocampus was indistinguishable in wild-type and heterozygous animals.

Histological and Immunological Analysis. To understand the basis for the various abnormalities observed in the affected heterozygous animals, the parts of the brain in which MAP1B was known to be expressed were examined at the histological level by light microscopy and by using antibodies directed against MAP1B, MAP1A, MAP2, and some neurofilament proteins. The changes that we observed are described below.

Histologically, abnormalities of the cerebellum were the most profound of all the areas affected in the brain. The most striking difference between wild-type and heterozygous animals was in the morphology of the Purkinje cells. Although the overall numbers of Purkinje cells were similar in the two groups of animals, cell bodies in the heterozygotes had lost their flask-shaped appearance (Fig. 2*c*) and appeared flattened (Fig. 2*d*).

To examine the basis for differences in Purkinje cell morphology, sections from wild-type and heterozygous animal brains were analyzed for MAP1B and MAP1A expression by using immunohistochemical methods. When antibodies directed against a nonnphosphorylated MAP1B epitope (designated 3G5) were used, the wild-type control showed a normal MAP1B staining pattern as well as normal-appearing Purkinje cell somata and dendrites (Fig. 3 *a* and *c*). The affected

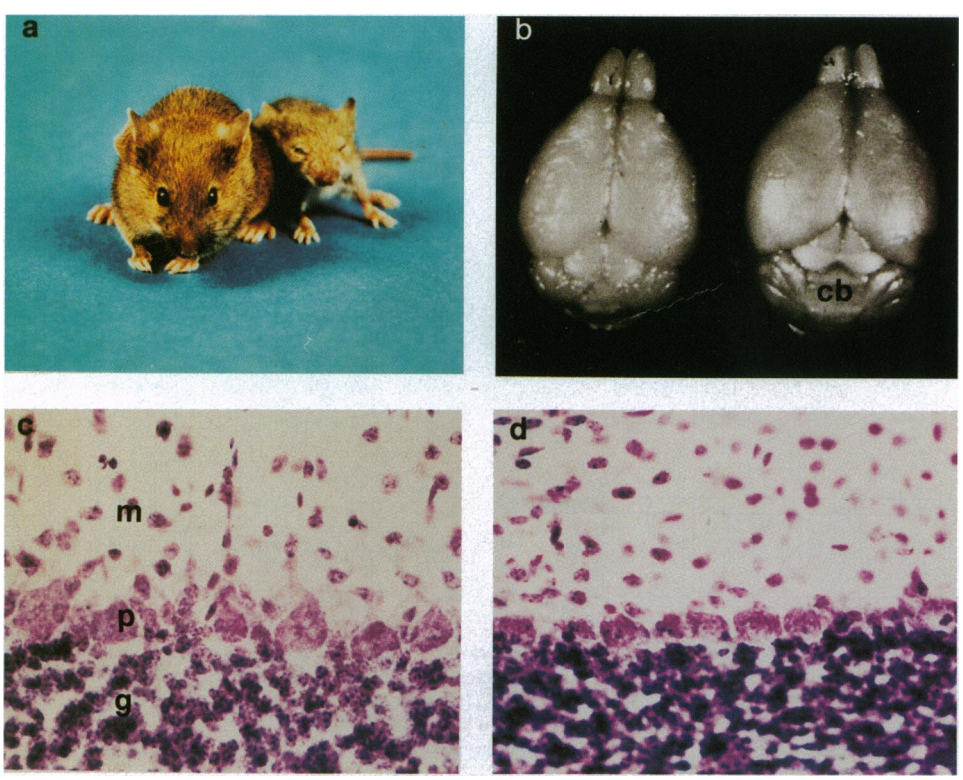

FIG. 2. Comparison of 5-month-old *Map1b571* heterozygote with its wild-type littermate. (*a*) Physical appearance of normal (left) and a severely affected *Map1b571* heterozygote (right). Note the small size, splayed hind leg posture, and severely underdeveloped eyes. (*b*) Comparison of brains from *Map1b571* heterozygote (left) and wild-type (right) animals; cb, cerebellum. (*c* and *d*) Purkinje cell morphology in wild-type (*c*) and *Map1b571* heterozygote (*d*); m, molecular layer; p, Purkinje cell layer; g, granular layer. (×1000.)

heterozygous animal, however, showed an overall lack of staining with the exception of a rare Purkinje cell (see Fig. 3 *b* and *d*). Similar results were obtained when we used antibodies directed against a phosphorylated epitope (designated 6D4; results not shown). When antibodies against MAP1A were used the Purkinje cells of heterozygous animals were found to have somewhat attenuated, truncated dendritic processes with decreased branching (see Fig. 3 *f* and *h*). Staining with antibodies directed against MAP2 (Fig. 4 *a* and *b*), another cytoskeletal protein expressed in Purkinje cells, revealed that these cells indeed have dendrites, although the branching of the dendrites is not as extensive as that in the wild-type animals.

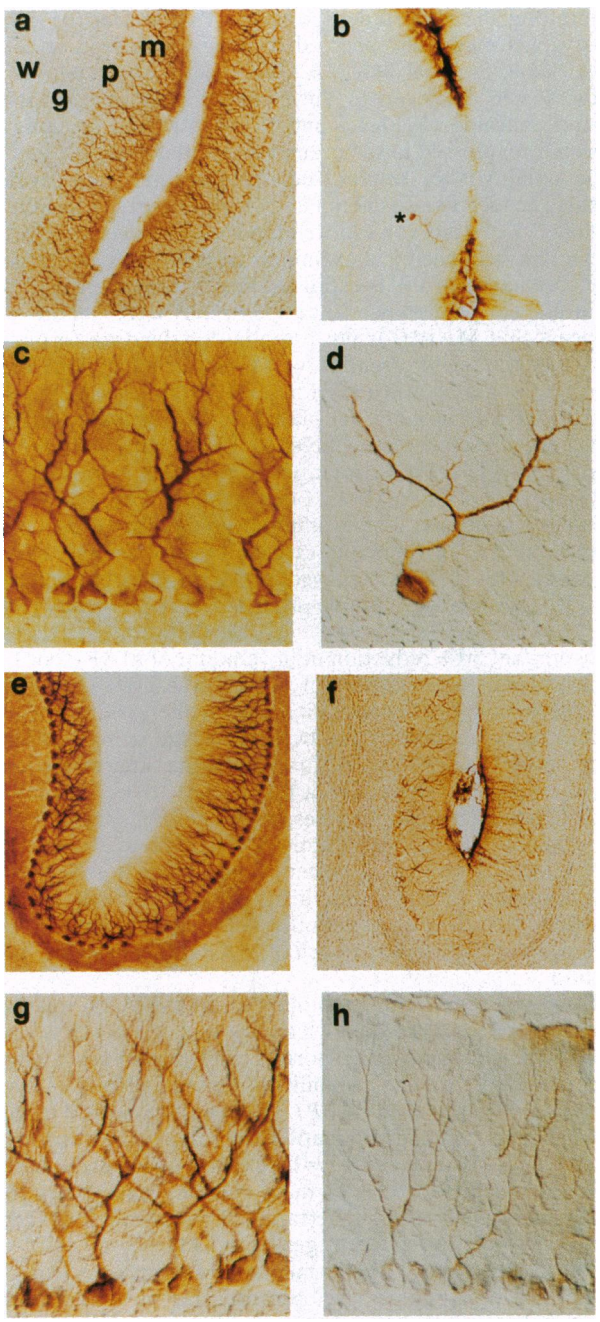

FIG. 3. Immunohistochemical analysis of brain sections from wild-type (*Left*) and *Map1b571* heterozygote (*Right*). (*a–d*) Staining with MAP1B-3G5 antibody; * marks a single Purkinje cell which reacted with the antibody; w, white matter; g, granular layer; p, Purkinje cell layer; and m, molecular layer. (*a* and *b*, ×250; *c* and *d*, ×1000.) (*e–h*) Staining with MAP1A antibody. (*e* and *f*, ×250; *g* and *h*, ×1000.)

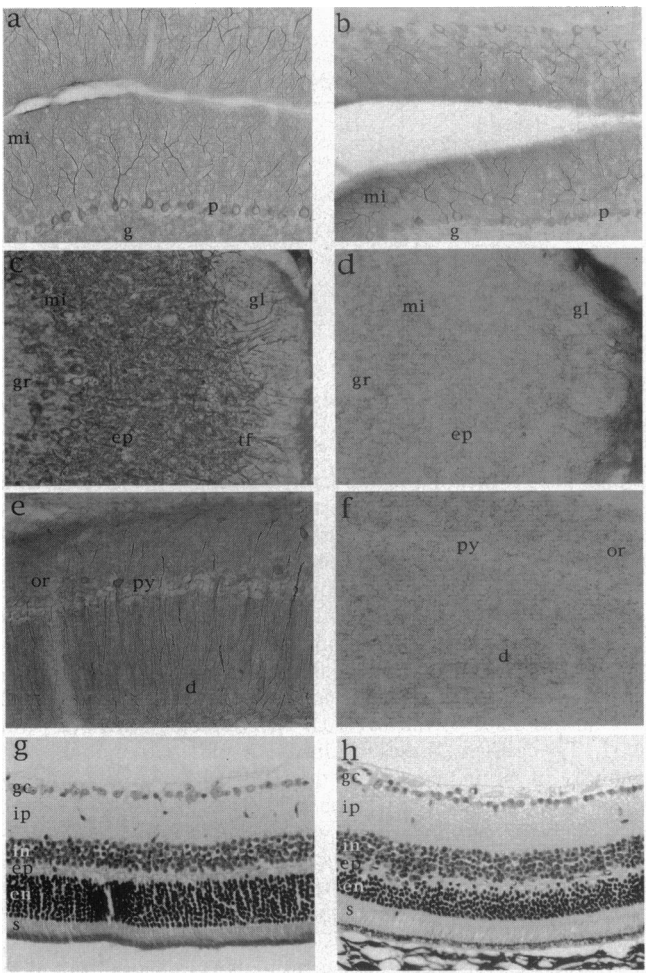

FIG. 4. Immunohistochemical analysis of brain sections from wild type (*Left*) and *Map1b571* heterozygote (*Right*). (*a* and *b*) Purkinje cells stained with MAP2 antibodies; mi, mitral layer; g, glomerular layer; p, Purkinje cells. (×720.) (*c* and *d*) Olfactory bulb stained with 6D4 antibody; gl, glomerular layer; ep, external plexiform layer; mi, mitral cell layer; tf, tufted cell layer; gr, granular layer. (×720.) (*e* and *f*) Hippocampus, CA1 region stained with 6D4 antibody; or, oriens layer; py, pyramidal cell layer; d, apical dendrites; hf, hippocampal fissure. (×720.) (*g* and *h*) Retina; gc, ganglion cell layer; ip, internal plexiform layer; in, internal nuclear layer; ep, external plexiform layer; en, external nuclear layer; s, inner and outer segments. (×720.)

When the olfactory tissue in normal animals was examined, the MAP1B antibodies moderately labeled the granular layer, the glomerular layer, and the olfactory nerve layer. Heavy labeling was observed in the external plexiform layer, the mitral cell layer, and the tufted cell layer, which had extensions into the glomeruli (Fig. 4*c*). The 6D4 antibodies revealed no such staining in the affected *Mab1b571* heterozygous animals (Fig. 4*d*).

Staining of the hippocampus in the wild-type animals with the 6D4 antibody revealed staining in the dendrites of all pyramidal cells (Fig. 4*e*) and an occasional cell body. No such staining was observed in the affected heterozygote (Fig. 4*f*).

Histological examination of the retina in the affected animals revealed that the internal nuclear layer as well as the external nuclear layer were disorganized compared with the wild-type littermates. We also observed a clear loss of demarcation of the external plexiform layer (Fig. 4 *g* and *h*).

The histochemical analysis suggested that despite the presence of a single functional copy of *Map1b*, the MAP1B expression pattern in several parts of the brain is profoundly affected. To determine the effect of the mutation on protein expression, we prepared cell extracts from brains of normal

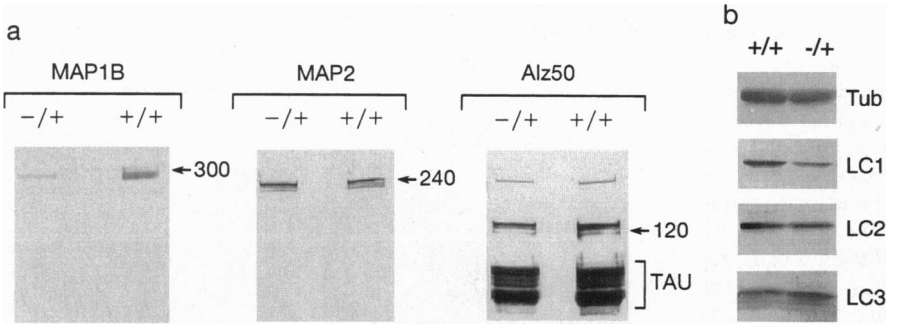

FIG. 5. (*a*) Expression of MAPs in normal and *Map1b571* heterozygous animals; −/+, heterozygote; +/+, wild type. Sizes of the proteins detected by the antibodies are indicated on the right of each panel in kDa. TAU refers to the protein forms corresponding to the MAP tau. (*b*) Expression of MAPs in the brain of normal and *Map1b571* heterozygotes; −/+, heterozygote; +/+, wild type; Tub, tubulin; LC, light chain.

and heterozygous animals and conducted immunoblot analysis using antibodies directed against MAP1B, the N-terminal 150 amino acids of MAP1B (MAP1B 489-3), MAP2 and Alz50, LC1, LC2, LC3, and tubulin. The Alz50 antibody reacts with all forms of tau, has some cross-reactivity to MAP2, and recognizes a 120-kDa protein termed FAC (18). The results are presented in Fig. 5. While the levels of tau and MAP2 proteins were unaltered in the heterozygotes, the level of MAP1B was reduced by about half as measured by 3G5 antibodies (Fig. 5*a*). A greater reduction in MAP1B was observed with the 6D4 antibodies, suggesting that phosphorylation of MAP1B is severely affected in *Map1b571* heterozygotes. No smaller polypeptide corresponding to the N-terminal 571 amino acids of the MAP1B was detected with 3G5 and 6D4. To confirm these results we conducted immunoblot analysis of brain extracts with MAP1B489-3, an antibody directed against the N-terminal 150 amino acids of MAP1B. Although this antibody is capable of detecting MAP1B protein, it did not detect the expected 64-kDa truncated protein. These results suggest that if a truncated protein is made from message derived from the *Map1b571* locus it is unstable. We examined the expression levels of the three light chains (LC1, LC2, and LC3) in heterozygous animals. Results presented in Fig. 5*b* show that LC1 levels are reduced while LC2 and LC3 levels are unaltered in the heterozygous animals.

***Map1b* Mutation Causes Embryonic Lethality in the Homozygous State.** *Map1b571* heterozygotes were interbred, and 200 F_2 offspring were genotyped for the modified *Map1b571* allele by Southern-blot analysis. Sixty of these animals were wild type and all of the remaining 140 animals were heterozygous for *Map1b571*. No animals carrying two *Map1b571* alleles were present among the 200 F_2 animals tested, suggesting that the modified *Map1b571* allele in the homozygous state results in embryonic lethality. To ascertain the stage of embryogenesis during which the gene modification results in lethality, we obtained embryos at different stages and genotyped them. Blastocyts (3.5-day embryos) included *Map1b571* homozygotes, but 8–8.5-day or 10.5-day embryos did not include any such homozygous animals. These results suggest that the *Map1b571* mutation, in the homozygous state, results in lethality sometime after the blastocyst stage but prior to day 8.5, which is referred to as the neural fold stage.

DISCUSSION

We introduced a mutation into the *Map1b* gene of the mouse. Mice which are heterozygous for this mutation, *Map1b571*, show a spectrum of growth and neuronal abnormalities, and the homozygous state results in embryonic lethality. Our data suggest that the *Map1b571* mutation is a null mutation. The reduced levels of MAP1B protein as well as LC1 protein together with the fact that we did not detect any truncated protein support this view. The observation that the mutation, in the homozygous state, results in embryonic lethality suggests that the MAP1B protein, LC1, or both are essential for normal development. Mature MAP1A and MAP1B share LC1, which is produced as a proteolytic product of MAP1B (4, 20). Therefore, the altered dosage of MAP1B in *Map1b571* heterozygotes might be expected to result in altered levels of MAP1B as well as MAP1A. We indeed observed such a reduction in the levels of these two proteins at least at the histochemical level (Figs. 3 and 4). Since MAP1 proteins are normally expressed in the brain, we postulate that the embryonic lethality is the result of failure of normal brain development. The fact that we did not detect any homozygous embryos at day 8.5 of embryonic development is consistent with this view. Our histochemical examination permits us to correlate the absence of MAP1B expression in Purkinje cells with the neurological phenotype. Since these cells have dendrites, it appears that MAP1B is not essential for dendrite formation but is nevertheless essential for normal cell function. These observations are consistent with the idea that MAP1B plays an important role in neuronal plasticity. The ocular phenotype observed in some of the heterozygous animals can be explained by the altered structure of the eye. It is possible that the absence of MAP1B in other parts of the brain (e.g., olfactory bulb and hippocampus) would also cause other abnormalities. Two possible explanations for the mechanism by which *Map1b571* heterozygotes exhibit the observed phenotypic characteristics can be proposed. One possibility is that the *Map1b571* mutation results in a null mutation such that the concomitant 50% reduction in the amount of MAP1B or LC1 is insufficient for assembly of normal MAP1B. The second alternative is that the mutation causes the production of a truncated polypeptide which by virtue of the presence of LC1 binding sites can prevent the function of the otherwise normal MAP1B protein derived from the normal allele. Despite the use of three different antibodies, one of which is specific for the N-terminal 150 amino acids of the MAP1B heavy chain, we did not detect any truncated protein. This makes it unlikely that the mutation acts in a dominant-negative fashion, and we conclude that the phenotypes that we observe are most likely the result of haploinsufficiency of MAP1B heavy chain, LC1, or both.

Mice with a mutation in another neuronal MAP, tau, have been described (21). Mice which are homozygous for a null mutation in this gene have a normal nervous system but exhibit occasional microtubule instability in some small-caliber axons. Increases in the levels of MAP1A have been observed in these tau-deficient mice. The dramatic differences in the phenotypes of the tau-deficient and *Map1b* mutant mice might reflect different functional roles of these proteins, and they underscore the importance of gene-targeted mice in understanding the *in vivo* roles of different gene products.

The availability of a *Map1b* mutant mouse provides a unique model for the study of developmental implications of mutations in the neuronal cytoskeleton on brain development and morphology and might provide clues to the etiology of human disorders in which these neuronal cell types are affected.

We thank Kirkland Lau, Xun Mei, Dong Liu, and Karin Haro for technical assistance, Drs. Steve Walkley, Patrick Stanton, and Jon Kwon for advice, Dr. Pearl Rosenbaum for histology of the eyes, and

Dr. Richard Vallee for critical review of the manuscript. The work described here was partially supported by the Human Genetics program at the Albert Einstein College of Medicine and by National Institutes of Health Grants HG00380 and HD31601 to R.K., AG09989 to N.C., and NIMH38623 to P.D. and by Cancer Center Grant CA13330 to the Albert Einstein College of Medicine. W.E. was a Deutsche Forschungsgemeinschaft Fellow.

1. Noble, M., Lewis, S. A., Cowan, N. J. (1989) *J. Cell Biol.* **109,** 3367–3376.
2. Bloom, G. S., Luca, F. C. & Vallee, R. B. (1985) *Proc. Natl. Acad. Sci. USA* **82,** 5404–5408.
3. Vallee, R. B. & Davis, S. E. (1983) *Proc. Natl. Acad. Sci. USA* **80,** 1342–1346.
4. Kutznetsov, S. A., Rodionov, V. I., Nadezhdina, E. S., Murphy, D. B. & Gelfland, V. I. (1986) *J. Cell Biol.* **105,** 1060–1066.
5. Hammerback, J. A., Obar, R. A., Hughes, S. A. & Vallee, R. B. (1991) *Neuron* **7,** 129–139.
6. Sato-Yoshitake, R., Shiomura, Y., Miyasaka, H. & Hirokawa, N. (1989) *Neuron* **3,** 229–238.
7. Riederer, B., Cohen, R. & Matus, A. (1986) *J. Neurocytol.* **15,** 763–775.
8. Garner, C. C., Garner, A., Huber, G., Kozak, C. & Matus, A. (1990) *J. Neurochem.* **55,** 146–154.
9. Schoenfeld, T. A., McKerracher, L., Obar, R. & Vallee, R. B. (1989) *J. Neurosci.* **9,** 1712–1730.
10. Tucker, R. P., Binder, L. I. & Matus, A. (1988) *J. Comp. Neurol.* **271,** 44–55.
11. Tucker, R. P. & Matus, A. (1987) *Development (Cambridge, U.K.)* **101,** 535–546.
12. Viereck, C., Tucker, R. P. & Matus, A. (1989) *J. Neurosci.* **9,** 3547–3557.
13. Calvert, R. & Anderton, B. H. (1985) *EMBO J.* **4,** 1171–1176.
14. Brugg, B. & Matus, A. (1988) *J. Cell Biol.* **107,** 643–650.
15. Mansfield, S. G., Diaz-Nido, J., Gordon-Weeks, P. R. & Avila, J. (1992) *J. Neurocytol.* **21,** 1007–1022.
16. Brugg, B., Reddy, D. & Matus, A. (1993) *Neuroscience* **52,** 489–496.
17. Mansour, S. L., Thomas, K. R. & Capecchi, M. R. (1988) *Nature (London)* **336,** 348–352.
18. Ksiezak-Redding, H., Davies, P. & Yen, S.-H. (1988) *J. Biol. Chem.* **263,** 7943–7947.
19. Mann, S. V. & Hammarback, J. A. (1994) *J. Biol. Chem.* **269,** 11492–11497.
20. Langkopf, A., Hammerback, J. A., Muller, R., Vallee, R. B. & Garner, C. C. (1992) *J. Biol. Chem.* **267,** 16561–16566.
21. Harada, A., Oguchi, K., Okabe, S., Kuno, J., Terada, S., Oshima, T., Sato-Yoshitake, R., Takei, J. & Hirokawa, N. (1994) *Nature (London)* **369,** 488–491.